A PRIORI STUDY OF THE STOCHASTIC MODEL FOR DISCRETE PHASE ACCELERATION IN A TEMPORALLY EVOLVING PLANAR JET USING DNS

Nabeel A. Qazi
School of Mechanical and
Manufacturing Engineering
The University of New South Wales
Sydney, 2052, NSW, Australia
n.qazi@unsw.edu.au

Haiou Wang
School of Mechanical and
Manufacturing Engineering
The University of New South Wales
Sydney, 2052, NSW, Australia
haiou.wang@unsw.edu.au

Michele Bolla
School of Mechanical and
Manufacturing Engineering
The University of New South Wales
Sydney, 2052, NSW, Australia
m.bolla@unsw.edu.au

Joshua C. K. Tang
School of Mechanical and
Manufacturing Engineering
The University of New South Wales
Sydney, 2052, NSW, Australia
joshua.tang@unsw.edu.au

Evatt R. Hawkes
School of Mechanical and
Manufacturing Engineering/
School of Photovoltaic and
Renewable Energy Engineering,
The University of New South Wales
Sydney, 2052, NSW, Australia
evatt.hawkes@unsw.edu.au

Ray W. Grout
National Renewable Energy
Laboratories
Computational Science Center
Colorado, USA
ray.grout@nrel.gov

ABSTRACT

This paper presents a priori study of the stochastic model for discrete phase acceleration using direct numerical simulation (DNS) results of a three-dimensional (3D), non-reacting, temporally evolving planar jet laden with mono-dispersed solid particles in the two-way coupling regime. The DNS database consists of two cases with particle Stokes number (St = 0.1, 1). The seen gas family of models (also referred as stochastic models) for particle acceleration in a Reynolds-Averaged-Navier-Stokes (RANS) context is studied here. Averaging of DNS data has been conducted in the streamwise and spanwise directions, simplifying the configuration into a temporally evolving statistically-one-dimensional (1D) case. 1D instantaneous mean and root mean square (r.m.s.) values of gas velocity across the jet have been used to reconstruct the instantaneous gas-phase velocities at particle locations according to the RANS-based stochastic model. Subsequently, DNS and modelled results are directly compared in terms of probability density functions of local instantaneous and relative velocities. Results indicate that the stochastic model fails to capture the correlation of particle and fluid velocities. This results in a much wider distribution of relative velocities which are required to calculate the particle accelerations. This is identified as potential source of model disagreement.

INTRODUCTION

Turbulent flows laden with solid particles are encountered in several engineering applications such as solar thermochemical systems, solid particle solar receivers, and coal/biomass combustion in power plants. In the last three decades, such flows have attracted much attention from both numerical and experimental perspectives as indicated by Balachandar & Eaton (2010). The most common numerical method employed to investigate such phenomena is the Eulerian-Lagrangian approach where particles are considered as point particles and are tracked using the Lagrangian equations, and the gas phase is regarded as a continuum. The key element of the Eulerian-Lagrangian approach is the way it accounts for the effects of turbulent fluctuations on the behavior and statistics of the discrete phase.

It is well understood that direct numerical simulation (DNS) uses the most accurate method to study such phenomena as all the turbulent scales are resolved without any modeling. However, certain limitations such as unavailability of ample computational resources has constrained DNS merely as a research tool. Hence, researchers opt for alternate options such as large-eddy simulation (LES) or Reynolds-averaged Navier-Stokes equations (RANS) methodologies to study these phenomena. In particular, RANS approach is most commonly used owing to its relatively low computational expense.

While utilizing direct numerical simulations, the instantaneous properties of the gas-phase can be directly interpolated at the particle locations, hence not requiring any approximations. The major challenge in using RANS approach is to model the turbulent properties of the flow field at particle locations. A stochastic approach is most commonly utilized where the turbulent flow is treated as a random field. Several models have been proposed under this assumption such as the classical seen-gas type model first presented by Gosman & Loannides (1983). Others include various random walk models for the diffusion of fluid particles by Thomson (1987) and Sawford (2001) and dispersion of solid particles in two-phase flows by Stock (1996) and Pozorski & Minier (1998). Moreover, a general probability density function (PDF) formalism has been developed as well (Reeks (1992) and Peirano *et al.* (2006)). Among these, the classical seen-gas type model, is still in use due its simplicity and ease of implementation. For example, it was more recently employed by Bermúdez *et al.* (2011) to study the group combustion of pulverized coal, and overprediction of particle dispersion was found upon comparison of numerical results with the experimental data.

A priori analyses of several models relating to particle acceleration have been carried out in the past but they were mostly devoted to isotropic turbulence in a periodic box (either forced and/or decaying) Pozorski & Apte (2009) and Cernick *et al.* (2015) primarily concentrated on the sub-grid scale modeling in the LES context. In particular, Cernick *et al.* (2015) report that the stochastic models tested in their work performed well in all the cases, but they were unable to successfully predict the preferential concentration. Similarly, the effect of spatial filtering and the role of subgrid scale turbulence on the statistics of heavy particles (including particle dispersion) were isolated via a priori analysis by Pozorski & Apte (2009). It was indicated that neglecting the influence of subgrid scale fluctuations had a significant effect on the preferential concentration. They also proposed a stochastic Langevin model to reconstruct the residual fluid velocity along the particle trajectories.

The goal of this work is to test the performance of the classical seen-gas model proposed by Gosman & Loannides (1983) in a jet configuration laden with non-reacting solid particles. The primary objective is to highlight the limitations of this stochastic model using DNS results and a priori analysis. The DNS database consists of a three-dimensional, non-reacting, temporally evolving planar jet laden with mono-dispersed solid particles. Two cases are are investigated by varying the particle diameter while keeping the mass loading ratio unvaried.

The remainder of the paper is organised as follows: firstly, a brief overview of the mathematical model is presented. This is followed by a short discussion on the basics of the seen-gas stochastic model. A section explaining numerical procedures and computational parameters is included as well. Results include flow statistics alongside probability density functions with explanations. Finally, concluding remarks are drawn.

MATHEMATICAL MODEL

In the current simulations, the gas-phase is regarded as Newtonian and compressible with the dispersed phase assumed dilute, which allows neglecting particle interaction. Two-way coupling in momentum and energy is however included. The particles are considered heavy such that only the Stokesian drag is considered and the rest of the terms are ignored along with gravity (Maxey & Riley (1983)).

In order to solve the set of equations that predict the evolution of non-interacting solid particles, three quantities are required. These include the location $\mathbf{x_p}$, velocity $\mathbf{U_p}$ and the fluid velocity $\mathbf{U_f}$ “seen” or sampled along a particle’s trajectory. In Eulerian-Lagrangian context, if $\mathbf{U}(\mathbf{x},\mathbf{t})$ is considered as the velocity field of the carrier phase then $\mathbf{U_f} = \mathbf{U}(\mathbf{x_p},\mathbf{t})$. Hence, governing equations for particle motion are:

$$\frac{d\mathbf{x_p}}{dt} = \mathbf{U_p} \tag{1}$$

$$\frac{d\mathbf{U_p}}{dt} = \frac{3}{4}\frac{\rho_f}{\rho_p}\frac{C_D}{d_p}|\mathbf{U_f}-\mathbf{U_p}|(\mathbf{U_f}-\mathbf{U_p}) \tag{2}$$

In Eq. (2), C_D is the drag coefficient based on particle Reynold number, $R_p = d_p|\mathbf{U_f}-\mathbf{U_p}|/\nu_f$, where d_p is the particle diameter and ν_f is the kinematic viscosity of the carrier phase. For most cases $R_p \leq 1000$ and the drag-coefficient is approximated via $C_D = (24/R_p)(1+0.15R_p^{0.687})$. The right hand side of Eq. (2) can be written in a simplified form as $(\mathbf{U_f}-\mathbf{U_p})/\tau_p$, written using the particle relaxation time $\tau_p = (\rho_p/\rho_f)d_p^2/18\nu_f$. ρ_f and ρ_p denote the density of carrier phase and dispersed phase respectively. The Stokes number of particles is defined as $St = \tau_p/\tau_j$, where τ_j is the characteristic time scale of the jet.

Stochastic Particle Dispersion Model

As mentioned earlier, while performing DNS with point particle approach, $\mathbf{U_f}$ can be directly calculated via interpolation of fluid velocities at the particle location. However, while considering RANS approach, $\mathbf{U_f}$ is obtained by coupling the particle motion equations with a stochastic model. The seen-gas model as proposed by Gosman & Loannides (1983) computes the instantaneous velocity as the sum of the mean fluid velocity and a Gaussian distributed random velocity fluctuations with zero mean and variance related to the turbulent velocity scale computed from the used turbulence model. Hence:

$$\mathbf{U_f} = \overline{\mathbf{U_f}} + \left(e_1\sqrt{\frac{2k}{3}}, e_2\sqrt{\frac{2k}{3}}, e_3\sqrt{\frac{2k}{3}}\right) \tag{3}$$

where e_i are normally distributed random numbers with zero mean and standard deviation of unity. If using the $k-\varepsilon$ model the eddy lifetime is expressed as :

$$\tau_e = -0.15\frac{k}{\varepsilon}log(r) \tag{4}$$

where r is a uniformly distributed random number between 0 and 1. More details can be found in the work carried out by Bermúdez *et al.* (2011).

NUMERICAL PROCEDURE

The flow configuration is a temporally-evolving planar slot-jet consisting of a slab of hot air, surrounded by air at lower temperature. The boundary condition for streamwise and spanwise directions is periodic, while in the lateral direction, the non-reflecting outflow boundary is selected.

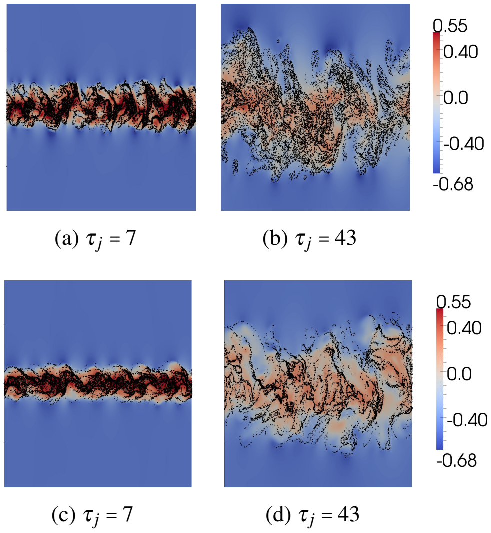

Figure 1: Instantaneous fluid velocity superimposed with particles at jet cross-section.(above): for St = 0.1, (below): for St = 1

Stretched grid is used in the lateral direction, whereas uniform grid is used in streamwise and spanwise directions. The DNS was performed using the massively parallel, FORTRAN based computer code, S3D which explicitly integrates the compressible, reacting Navier-Stokes equations. The numerical solution is advanced in time by employing a fourth order, six-stage, low-storage Runge-Kutta method. An eighth order central difference scheme is utilised for spatial derivatives on a three dimensional Cartesian grid (Hawkes *et al.* (2005)). The particle equations are solved through Particle Source in Cell (PSI-Cell) method (Crowe *et al.* (1985)). The particles are assumed to distribute randomly in the jet area with initial temperature and velocity regarded same as the local fluid. The local properties of the fluid are interpolated at the particle locations using fourth order Lagrangian interpolation scheme. For efficiency purposes, computational particle approach was adopted; where a single computational particle represents a collection of real particles with the same properties. Particle Stokes number is varied from 0.1 to 1 by changing the particle diameter and decreasing the number of particles to retain the same mass loading, whereas all other parameters are kept constant. Further details and information regarding DNS parameters can be found in our previous work (Qazi *et al.* (2014)).

RESULTS AND DISCUSSION

The results include the effects of particle feedback on flow field, velocity profiles for mean fluid velocity and r.m.s. of velocity fluctuations. Lastly, comparison has been made via pdfs and joint pdfs for instantaneous fluid velocities at particle locations for DNS and RANS based stochastic model. In the following, the velocities have been normalised by the initial difference of velocity between the jet and the co-flow.

Flow Statistics

Figure 1 shows the contours of the velocity of the carrier phase, normalised by velocity difference, ΔU, superimposed with particles in a typical x-y plane. Initially, particles in both cases are spread homogeneously in the domain. As the simulation progresses, fluctuations in the shear regime of the jet cause increase of vortical structures and the spreading of jet takes place. Figures 1a and 1b show that for St = 0.1 the jet has spread farther in the lateral direction as compared to St = 1. The clustering mechanisms are different in both cases as well. For lighter particles (St = 0.1), the particles follow the flow closely and are generally homogeneously distributed in the domain, with partial clustering visible. However, in the case of heavier particles, it is shown that they preferentially concentrate in the outer boundaries of large-scale vortex structures. This can be clearly observed in Fig. 1d. Such a qualitative comparison between the width of the jet for the two cases, at same time stamps indicate the suppression of fluid fluctuations due to presence of laden particles. This is in compliance with similar works carried out in the past Yan *et al.* (2008) and Gui *et al.* (2013)

Figure 2 illustrates the profiles of normalized mean axial velocities, $< u >$, for the two cases. Here, $<>$ denotes the ensemble averaging performed in streamwise and spanwise direction for each lateral location. It is suggested that the presence of particles augments the mean streamwise velocity in the center of the jet whereas it is attenuated towards the edges. Moreover, this degree of modification increases with the increase in Stokes number. The transfer of momentum between the two phases is considered responsible

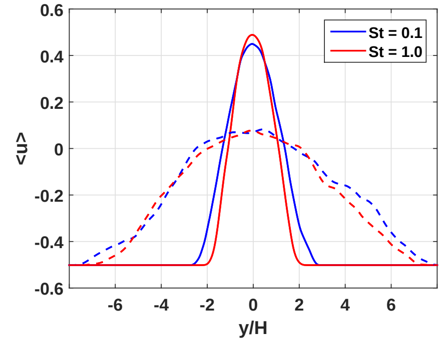

Figure 2: Effect of particle feedback on the mean velocity profiles of fluid. (solid) $\tau_j = 7$; (dashed) $\tau_j = 43$.

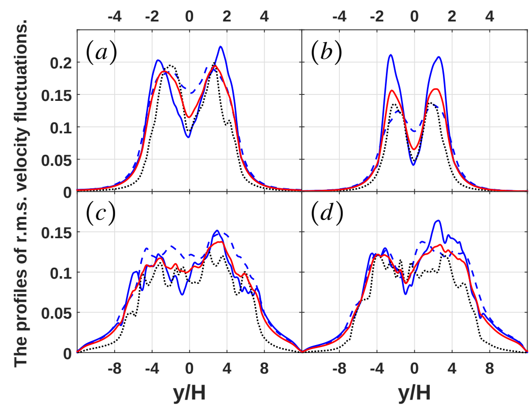

Figure 3: The profiles for r.m.s. velocity fluctuations. (left): St = 0.1, (right): St = 1. (above): $\tau_j = 7$, (below): $\tau_j = 43$. (—) u', (- - -) v', (. . .) w', (—) k^*

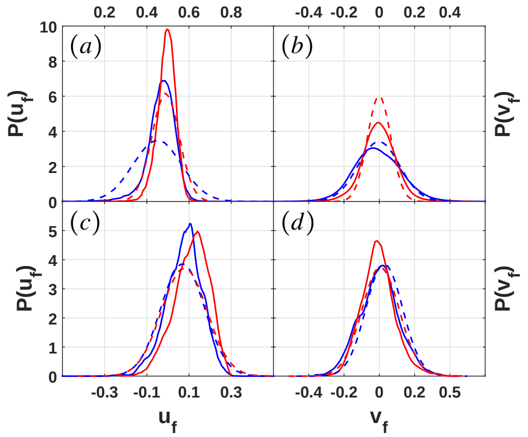

Figure 4: PDF of instantaneous velocities at central location. (above): $\tau_j = 7$, (below): $\tau_j = 43$. (—) $St = 0.1_{,\,DNS}$; (- - -) $St = 0.1_{,\,model}$; (—) $St = 1_{,\,DNS}$; (- - -) $St = 1_{,\,model}$.

for this phenomenon (Luo *et al.* (2005)).

The profiles for r.m.s. of velocity fluctuations of the carrier phase are presented in Fig. 3. At $\tau_j = 7$, (see Fig. 3a and b) the axial fluctuations dominate in the shear regime whereas the central region is dominated by the fluctuations in the lateral direction. These effects are more dominant for the case where the flow is laden with particles of St = 1. Additionally, the assumption of isotropic turbulence may not be valid in this scenario.

At $\tau_j = 43$ however, (see Fig. 3c and d), the difference between the fluctuating velocity components is not so stark. This is expected, owing to the fact that as jet develops, the turbulence tends to have more isotropic and homogeneous characteristics.

The profiles for k^*, where $k^* = \sqrt{2k/3}$ and $k = 0.5 \times (u'^2 + v'^2 + w'^2)$ are also included in Fig. 3. As briefed earlier, they are required to reconstruct the velocity fluctuations at particle locations according to RANS based stochastic model.

Central Layer

Probability density functions have been extracted for local instantaneous velocity of the carrier phase seen at particle locations from the DNS database at central and shear locations and compared with the model. It is found that the stream-wise fluid velocity obtained from DNS has a general Gaussian distribution, however it is slightly skewed towards the right. On the other hand, the instantaneous velocities obtained from the model have a wider distribution while still strictly following the assumed Gaussian profile. Contrasting effects are observed for the velocities in lateral direction. For the lateral direction, the stochastically modeled velocities have a narrower distribution as compared to actual DNS values for both Stokes number cases. This behavior can be explained by inspecting Fig. 3 in detail. It is seen that at the center of the jet, k^* is larger than u' but smaller than v'. This shall have a direct impact while randomly obtaining fluctuating velocities using Eq. (3). It is noted that the prediction of the most probable velocities via stochastic model is in good agreement with DNS values.

At $\tau_j = 43$, the model prediction is relatively better. By this time, the jet has developed and the difference between

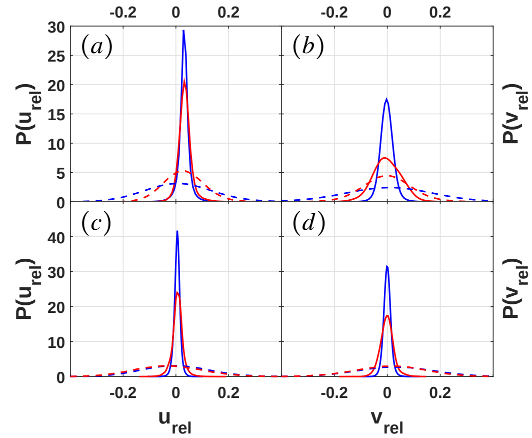

Figure 5: PDF of relative velocities at central location. (above): $\tau_j = 7$, (below): $\tau_j = 43$ (—) $St = 0.1_{,\,DNS}$; (- - -) $St = 0.1_{,\,model}$; (—) $St = 1_{,\,DNS}$; (- - -) $St = 1_{,\,model}$.

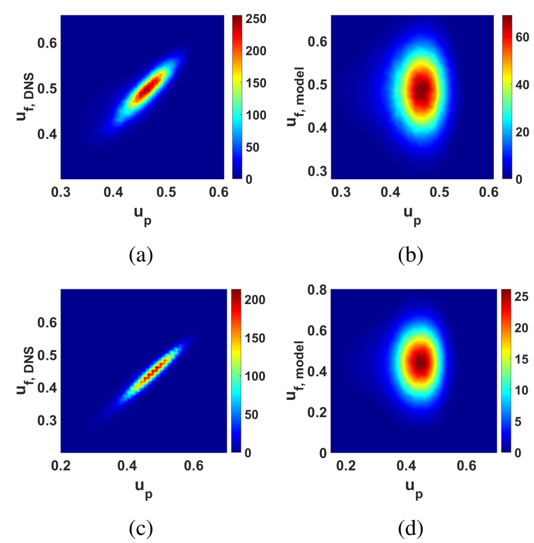

Figure 6: Contours of joint PDF of instantaneous velocities at central location at $\tau_j = 7$. (above): St = 1, (below): St = 0.1

the profiles is not so apparent, as evident from Fig. 3. In this scenario, the assumption of isotropic turbulence is more valid, where $u' \approx v' \approx w' \approx \sqrt{2k/3}$.

According to Eq. (2), it is seen that the most dominant factor in the calculation for acceleration of particle is the relative velocity. In Fig. 5, the pdf of relative velocity components in streamwise and lateral direction are presented. From the figures, the difference between the distribution of relative velocities is apparent. The distribution for relative velocities obtained from stochastic model are wider in all cases, while being much wider for St = 0.1 case for $\tau_j = 7$. This difference is pronounced at later time, $\tau_j = 43$, while being indistinguishable for both St = 1 and St = 0.1 for stochastically modeled velocities.

This suggests that the velocity of particles may be correlated with the local instantaneous fluid velocity. Such a correlation is inherently ignored when a Gaussian distribution is assumed for the RANS context. To investigate this further,

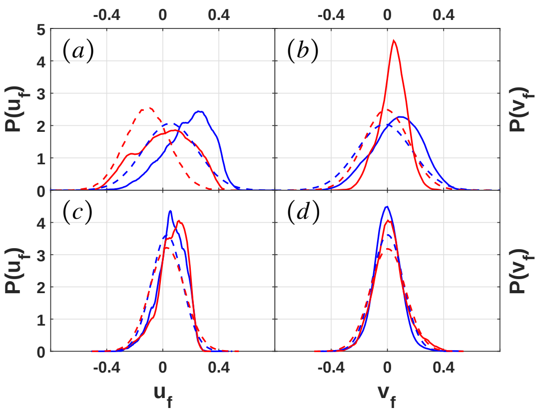

Figure 7: PDF of instantaneous velocities at location of shear layer. (above): $\tau_j = 7$, (below): $\tau_j = 43$ (—) $St = 0.1_{,\ DNS}$; (- - -) $St = 0.1_{,\ model}$; (—) $St = 1_{,\ DNS}$; (- - -) $St = 1_{,\ model}$.

the contours of joint pdf of particle velocities with the fluid velocity seen at particle locations in stream-wise direction are presented in Fig. 6. The positive correlation of particle velocities with the carrier phase velocity is evident. This correlation is much stronger in St = 0.1 case as they behave almost like flow tracers and follow the flow more closely than the more inertial St = 1 particles. While the model predicts the most probable relative velocity quite close to DNS, the distributions are wider for the model. As a consequence, the particle acceleration may be very different from that of DNS. This results in incorrect depiction of characteristics of the discrete phase. Therefore, care should be taken while using such a model for RANS based calculations in similar configurations.

Shear Layer

The performance of the stochastic model is slightly inferior in the shear layer for initial time. From Fig. 7 it can be observed that the model predicts the velocity slightly lower than the actual DNS values. Furthermore, the Gaussian shape is still maintained but the skewness of pdf of velocities from DNS is not accurately captured. This behavior can again be understood by inspecting Fig. 3. It is depicted that in the shear regime, u' is the dominant factor while v' has the least value.

At $\tau_j = 43$, the profiles show slightly better comparison for lateral component of the instantaneous velocity, which was observed for central location as well. From Fig. 3(c and d) it can be observed that in the shear regime, the values of fluctuating components and that of turbulent kinetic energy fluctuations as calculated from DNS are quite close.

Despite the fact that when using the stochastic model, the instantaneous velocities are predicted close to DNS values, the actual difference intensifies for the calculation of relative velocities. This is true for both central and shear location, and for both tracer like (St = 0.1) and inertial (St = 1) particles. (The shape of pdf of relative velocities for this case were similar to that of central layer (see Fig. 5), and therefore have not been included here.) Once again, it is stressed that this variation appears due to intrinsic properties of the stochastic model, hence ignoring the correlation of the velocities of the two phases which is evident from actual DNS simulations. To clarify this argument, we present the joint pdfs of the velocity two phases in the shear regime

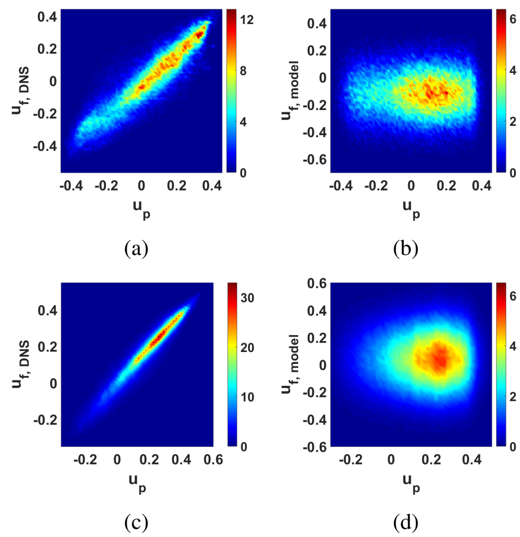

Figure 8: Contours of joint PDF of instantaneous velocities in the shear regime at $\tau_j = 7$. (above): St = 1, (below): St = 0.1

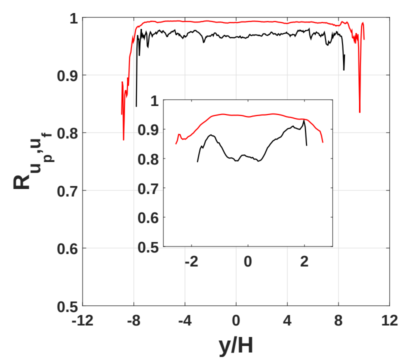

Figure 9: Spatial evolution of Lagrangian correlation factor at $\tau_j = 43$ from DNS database. (—) $St = 0.1$; (—) $St = 1$. The inset presents results at $\tau_j = 7$.

in Fig. 8.

As noted for the central location, the positive slope of the relationship indicates strong correlation between the velocities. Even though the prediction of the instantaneous velocities have good agreement between DNS and stochastic model, the joint pdf in RANS case depicts a slope almost equal to zero. As before, the correlation is stronger in the case of tracer like particles, which adopt to the local flow properties quicker than the inertial particle (St = 1). Furthermore, this relationship is expected to increase in strength as the jet develops and turbulent characteristics start to take hold. The lighter particles will settle abruptly to the varying conditions they are exposed to, whereas the inertial particles shall still contain memory of their interaction with the previous eddy.

Velocity Correlations Between Particles and Fluid

The Lagrangian correlation factor defined as: $R_{u_p,u_f} = \langle u'_p u'_f \rangle / \langle {u'_p}^2 \rangle^{1/2} \langle {u'_f}^2 \rangle^{1/2}$ has been calculated from DNS database. The spatial evolution of R_{u_p,u_f} for $\tau_j = 43$

is shown in Fig. 9. The inset presents the profiles for $\tau_j = 7$ as well. The results confirm the general impression of statistical relationship between the data set provided by the contours of joint pdf in figures 6 and 8. At $\tau_j = 7$, it is seen that the correlation between the particle and fluid velocities is almost close to 1, hence indicating strong dependence on the conditions around particle location. On the other hand, this dependance is not as strong for the case of inertial particles (St = 1). As expected, the dependence strengthens as the jet develops with time. At $\tau_j = 43$, the correlation factor is approximately equal to 1 for both cases. Slight demarcation can still be observed between the two cases where particles of varying relaxation time are exposed to different surrounding conditions.

CONCLUSION

Direct numerical simulation has been performed for a three-dimensional particle-laden planar jet in the two-way coupling regime. Two cases are considered, tracer like particles (St = 0.1) and inertial particles (St = 1). The DNS database is used to generate mean and r.m.s. statistics for the flow field. The averaging has been performed in streamwise and spanwise direction to obtain 1D statistics for a priori analysis in RANS context. The classical seen-gas type stochastic model as applied in RANS context is tested via a priori analysis. The mean and r.m.s. statistics from DNS are used to reconstruct the instantaneous fluid velocities at the particle locations. The performance of the model has been tested through pdf and joint pdfs of local particle and fluid velocities. Results indicate that although the stochastic model is able to predict the distribution instantaneous fluid velocities close to DNS, it fails to take into account the lagrangian correlation between the two phases. As a result, the distribution of relative velocities is much wider as compared to expected DNS distribution. This is identified as the main contributor to over prediction of particle characteristics as reported in recent literature.

ACKNOWLEDGEMENT

The research was performed using computational resources sponsored by the Department of Energy's Office of Energy Efficiency and Renewable Energy, located at the National Renewable Energy Laboratory. It also benefited from computational resources provided through Department of Energy Office of Advanced Scientific Computing Research, the National Computational Merit Allocation Scheme, supported by the Australian Government and Australian NCI National Facility, the partner share of the NCI facility provided by Intersect Australia Pty Ltd., the Peak Computing Facility of the Victorian Life Sciences Computation Initiative (VLSCI), iVEC (Western Australia), and the UNSW Faculty of Engineering.

REFERENCES

Balachandar, S & Eaton, John K 2010 Turbulent dispersed multiphase flow. *Annual Review of Fluid Mechanics* **42**, 111–133.

Bermúdez, A., Ferrín, J. L., Liñán, A. & Saavedra, L. 2011 Numerical simulation of group combustion of pulverized coal. *Combustion and Flame* **158** (9), 1852–1865.

Cernick, M. J., Tullis, S. W. & Lightstone, M. F. 2015 Particle subgrid scale modelling in large-eddy simulations of particle-laden turbulence. *Journal of Turbulence* **16** (2), 101–135.

Crowe, CT, Gore, RA & Troutt, TR 1985 Particle dispersion by coherent structures in free shear flows. *Particulate Science and Technology* **3** (3-4), 149–158.

Gosman, A. D. & Loannides, E. 1983 Aspects of computer simulation of liquid-fueled combustors. *Journal of Energy* **7** (6), 482–490.

Gui, N., Yan, J., Fan, J. & Cen, K. 2013 A dns study of the effect of particle feedback in a gas–solid three dimensional plane jet. *Fuel* **106**, 51–60.

Hawkes, E R, Sankaran, R, Sutherland, J C & Chen, J H 2005 Direct numerical simulation of turbulent combustion: fundamental insights towards predictive models. In *Journal of Physics: Conference Series*, , vol. 16, pp. 65–79. IOP Publishing.

Luo, K., Fan, J. & Cen, K. 2005 Modulations on turbulent characteristics by dispersed particles in gas–solid jets. *Proceedings of the Royal Society A: Mathematical, Physical and Engineering Science* **461** (2062), 3279–3295.

Maxey, M. R. & Riley, J. J. 1983 Equation of motion for a small rigid sphere in a nonuniform flow. *Physics of Fluids (1958-1988)* **26** (4), 883–889.

Peirano, E., Chibbaro, S., Pozorski, J. & Minier, J-P. 2006 Mean-field/pdf numerical approach for polydispersed turbulent two-phase flows. *Progress in energy and combustion science* **32** (3), 315–371.

Pozorski, J. & Apte, S. V. 2009 Filtered particle tracking in isotropic turbulence and stochastic modeling of subgrid-scale dispersion. *International Journal of Multiphase Flow* **35** (2), 118–128.

Pozorski, J. & Minier, J-P. 1998 On the lagrangian turbulent dispersion models based on the langevin equation. *International Journal of Multiphase Flow* **24** (6), 913–945.

Qazi, N. A., Tang, J. C. K., Hawkes, E. R., Yeoh, G. H., Grout, R. W., Sitaraman, H., Talei, M., Taylor, R. A., Bolla, M. & Wang, H. 2014 Direct numerical simulation of particle behaviour in a gas-solid three dimensional plane jet. *19th Australasian Fluid Mechanics Conference, Melbourne, Australia* (Paper ID: 389).

Reeks, MW 1992 On the continuum equations for dispersed particles in nonuniform flows. *Physics of Fluids A: Fluid Dynamics (1989-1993)* **4** (6), 1290–1303.

Sawford, B. 2001 Turbulent relative dispersion. *Annual review of fluid mechanics* **33** (1), 289–317.

Stock, D. E. 1996 Particle dispersion in flowing gases1994 freeman scholar lecture. *Journal of fluids engineering* **118** (1), 4–17.

Thomson, D. J. 1987 Criteria for the selection of stochastic models of particle trajectories in turbulent flows. *Journal of Fluid Mechanics* **180**, 529–556.

Yan, J., Luo, K., Fan, J., Tsuji, Y. & Cen, K. 2008 Direct numerical simulation of particle dispersion in a turbulent jet considering inter-particle collisions. *International Journal of Multiphase Flow* **34** (8), 723–733.